*Int. J. Electrochem. Sci.*, 10 **(2015)** 5737 - 5746

International Journal of
ELECTROCHEMICAL
SCIENCE
www.electrochemsci.org

# Synthesis of $Pt_xPd_y$ Nanoparticles Decorated Functionalized Carbon Nanotubes as Highly Anodic Catalysts for Formic Acid Fuel Cells

*Suwaphid Themsirimongkon*[1], *Thapanee Sarakonsri*[1,2], *Somchai Lapanantnoppakhun*[1,3], *Surin Saipanya*[1,2,*]

[1]Department of Chemistry, Faculty of Science, Chiang Mai University, Chiang Mai, 50200 Thailand
[2]Materials Science Research Center, Faculty of Science, Chiang Mai University, 50200 Thailand
[3]Center of Excellence for Innovation in Analytical Science and Technology, Chiang Mai University, 50200 Thailand
[*]E-mail: surin_saipanya@hotmail.co.uk

*Received:* 26 August 2014 / *Accepted:* 18 March 2015 / *Published:* 27 May 2015

$Pt_xPd_y$ catalysts with various compositions onto functionalized carbon nanotubes (CNTs) were prepared by improved polyol method to study their electrocatalytic activities toward a formic acid oxidation. Carbon nanotubes as supports (CNTs) were functionalized by acid solutions and the different atomic weight ratios of Pt to Pd supported the functionalized CNTs were prepared. X-ray diffraction (XRD) and transmission electron microscopy (TEM) were used to investigate the catalyst morphologies and particle size distributions. A uniform dispersion of alloyed microstructure $Pt_xPd_y$ particles with diameters ranging between 2-4 nm was obtained. The effect of different surface compositions of various $Pt_xPd_y$ /CNTs alloy particles on electrocatalytic formic acid oxidation were investigated by cyclic voltammetry (CV) and chronoamperometry (CA). The results showed an excellent activities and stabilities which are indicated by its lower onset potential and higher current density. Moreover, the PdPt/CNTs catalyst was obtained higher superior electrocatalytic activity than the other $Pt_xPd_y$ catalysts and the commercial PtRu/C.

**Keywords:** Direct formic acid fuel cell; Anode catalyst; Improved polyol method

## 1. INTRODUCTION

An exploration for new energy sources is crucial as limits of fossil fuel reserve and environmental concerns nowadays. Low-temperature fuel cells can be used varieties of fuels such as hydrogen, methanol, ethanol, formic acid or other hydrocarbons. Those small organic molecules have low-molecular mass and directly oxidize to produce a power [1,2]. Formic acid has recently attracted

our interest for fuel cells as its higher theoretical open circuit voltage and lower fuel cross-over compared with methanol [1,3,4]. Formic acid oxidation takes place through an accepted duel pathway mechanism: One of the paths produces $CO_2$ through an active intermediate (Dehydrogenation) and the other parallel path, $CO_2$ is formed through a poisonous intermediates with oxygen containing species e.g. CO, HCO and HCOOH leading to $CO_2$ (Dehydrogenation).

A simple and successful alternative to reduce the CO poisoning effect is addition of supporting elements to Pt [1,5,6]. The additive elements provide the generation of oxygen containing species at low potentials compared with monometallic Pt. This phenomenon is called bifuntional mechanism, where the intermediate e.g. $CO_{ads}$ react with hydroxilated species. It should be stated that palladium (Pd) has a good electrocatalytic activity towards formic acid oxidation as lesser amount of formed $CO_{ads}$ and lower onset potential [6-9].

Moreover, supporting material is important as it can affect the electrochemical activity of metallic catalysts. Carbon nanotubes (CNTs) are one of the promising catalyst support candidates for low-temperature fuel cells as their unique structures and properties such as high-surface area, good electronic conductivity, strong mechanical property and high-chemical stability [9-11]. Modification of CNTs surface by acid treatment [10-13] before loading the catalyst nanoparticles and development of catalyst preparation method to control the size and distribution of metallic nanoparticles on the CNTs are our research.

In this work, the CNTs supports were functionalized by acid solution and use of the improved polyol method to prepare of metal nanoparticles (mono and bimetallic) were simply achieved to load the metal catalyst with small size and well dispersibility on the functionalized CNTs. The electrochemical characteristics and electrocatalytic activities of $Pt_xPd_y$ /CNTs with various atomic ratio catalysts were examined for formic acid oxidation aiming for applications in direct formic acid fuel cell.

## 2. EXPERIMENTAL SECTION

### *2.1. Chemicals*

Multiwalled carbon nanotubes (CNTs; Bayer tubes C150P) were employed as support materials. Hexachloroplatinic acid hexahydrate ($H_2PtCl_6.6H_2O$; 40%), palladium (II) chloride ($PdCl_2$; 59%), nitric acid ($HNO_3$; 65%), sulfuric acid ($H_2SO_4$; 97%) and sodium hydroxide (NaOH; 95%) were obtained from Merck. Formic acid (HCOOH; 99.6%) was received from Fischer Chemical. Ethylene glycol ($C_2H_6O_2$; 99.5%) was purchased from Ajax Finechem. Deionized water was obtained from a Millipore Milli-Q water system.

### *2.2. Synthesis of mono and di $Pt_xPd_y$/CNTs electrocatalysts*

To modify surfaces area of the supporting material, the CNTs were functionalized using 2.6 M $HNO_3$ at 60-90 $^{\circ}$C for 24 h. The oxidized CNTs suspension was separated by centrifugation, washed with deionized water until neutral pH and then dried in an oven at 60 $^{\circ}$C (labeled as CNTs).

10 wt.% metal content with different atomic ratios (labeled as Pt, Pd and $Pt_xPd_y$/CNTs catalysts) were prepared by an improved polyol method. Briefly, $H_2PtCl_6.6H_2O$ and/or $PdCl_2$ precursors were dissolved in ethylene glycol: water (3:1). The functionalized CNTs were ultrasonically dispersed in ethylene glycol (EG) solution for 30 min at room temperature and the Pt and/or Pd precursor solutions were dropped under mechanical stirring at 1300 rpm to the dispersed CNTs in EG suspension. Then the pH of the solution was adjusted to approximately 11 by slowly dropping 1 M NaOH solution while stirring at 1300 rpm and heating up to 120 $^{\circ}$C. After that, the solutions were refluxed and maintained with this condition for 3 h. Finally, the solutions were cooled to room temperature and washed several times with deionized until the pH reached neutral and the obtained catalysts were dried in an oven at 60 $^{\circ}$C overnight.

### *2.3. Electrocatalyst Characterizations*

An X-Ray Diffractometer (D/MAX-2500/PC, Rigaku Co., Japan), equipped with a Cu Kα source in the range of $2\theta = 10 - 80$, was used to identify structural characteristics the catalysts. The particle size was measured utilizing the Debye-Scherrer equation [14].

Transmission electron microscopy (TEM; JEOL, JEM-2010) at a 200 kV expediting voltage was used for examining the size distribution of the catalyst nanoparticles on the functionalized CNTs supports. For sample preparation, few amount of the catalyst were dispersed in ethanol under ultrasonication and then the suspension were dropped onto copper grid for several times and then dried under the lamp.

### *2.4. Electrochemical measurements*

A conventional three-electrode electrochemical cell, at the ambient temperature was performed for all electrochemical measurements. The three electrode cell system consisting of a Ag/AgCl (3.5 M KCl) and a platinum wire are reference and counter electrodes, respectively. The working electrode (3 mm in diameter) was modified by a thin layer of catalyst inks. Before use the working electrode was polished with alumina slurries. The catalyst ink was prepared as following details: 5 mg catalyst, 900 µl of DI-water, 400 µl of Nafion (5 wt % ), 400 µl of ethanol, and 1,000 µl of phosphate buffer solutions were ultrasonically mixed, then dropped 7 µl of this ink onto the polished glassy carbon electrode and left it to be dried under the lamp.

A potentiostat (eDAQ) was used for the electrochemical measurements. The electrochemical active surface area (ECSA) of the catalysts was measured in 0.5 M $H_2SO_4$ solution and calculated from hydrogen desorption curves, which was recorded -0.4 and 1.0 V region. The activities of the catalyst electrodes for formic acid oxidation were measured in nitrogen saturated 0.5 M HCOOH in 0.5 M $H_2SO_4$ solution at -0.2 and 1.0 V with scan rate was set at 50 $mV.s^{-1}$. In order to measure the durability of the prepared catalysts electrodes, chronoamperometric (CA) measurements were carried out in 0.5 M HCOOH in 0.5 M $H_2SO_4$ at 0.4 V for 3600 s.

## 3. RESULTS AND DISCUSSION

### *3.1. Catalyst Characterizations*

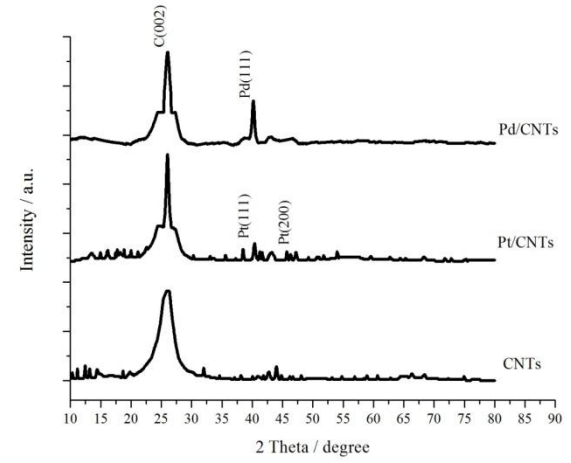


(a)

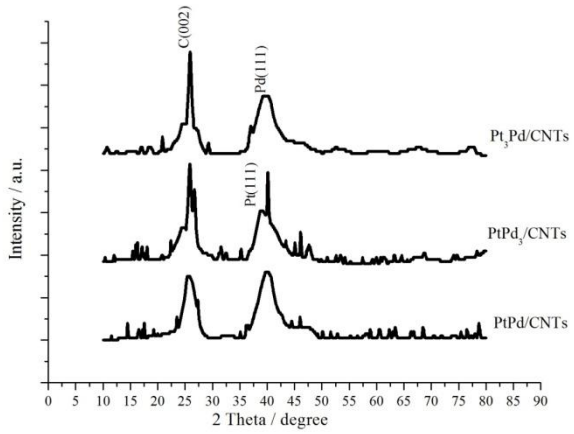


(b)

**Figure 1.** Powder X-ray diffraction patterns of a) monometallic catalysts : CNTs, Pt/CNTs and Pd/CNTs and b) dimetallic catalysts : PtPd/CNTs, $PtPd_3$/CNTs and $Pt_3Pd$/CNTs.

The XRD patterns of all catalysts in this study are shown in Figure 1. The first peaks of all catalyst ca. 25.2° correspond to (200) crystal face of the functionalized CNTs carbon supports [15]. It is valuable to point out those peaks have sharp diffraction peaks which could explain that they have high degree of graphitization and could improve the electric conductivity of the catalysts. Therefore, it is consistently observed in all catalyst patterns [10]. Moreover, all of them show the main characteristic patterns of Pt face-centered cubit (fcc) crystalline structures at 2θ at 39.77°and 46.24° which are matched up with Pt(111) and Pt(200) respectively [16, 17]. It is disclosed that XRD patterns are proven that the catalyst particles have the fcc structure and the Pt and Pd on functionalized CNTs catalysts formed a solid solution. The XRD peak of (111) plane of pure Pt and Pd are obtained at 39.77° and 40.40°, respectively [17]. However, the XRD peak of (111) plane of PtPd/CNTs lies in

between the range of Pt and Pd nanoparticles. The shift in (111) peak position in relation to Pt/CNT confirms the alloy formation in the PtPd/CNT catalysts.

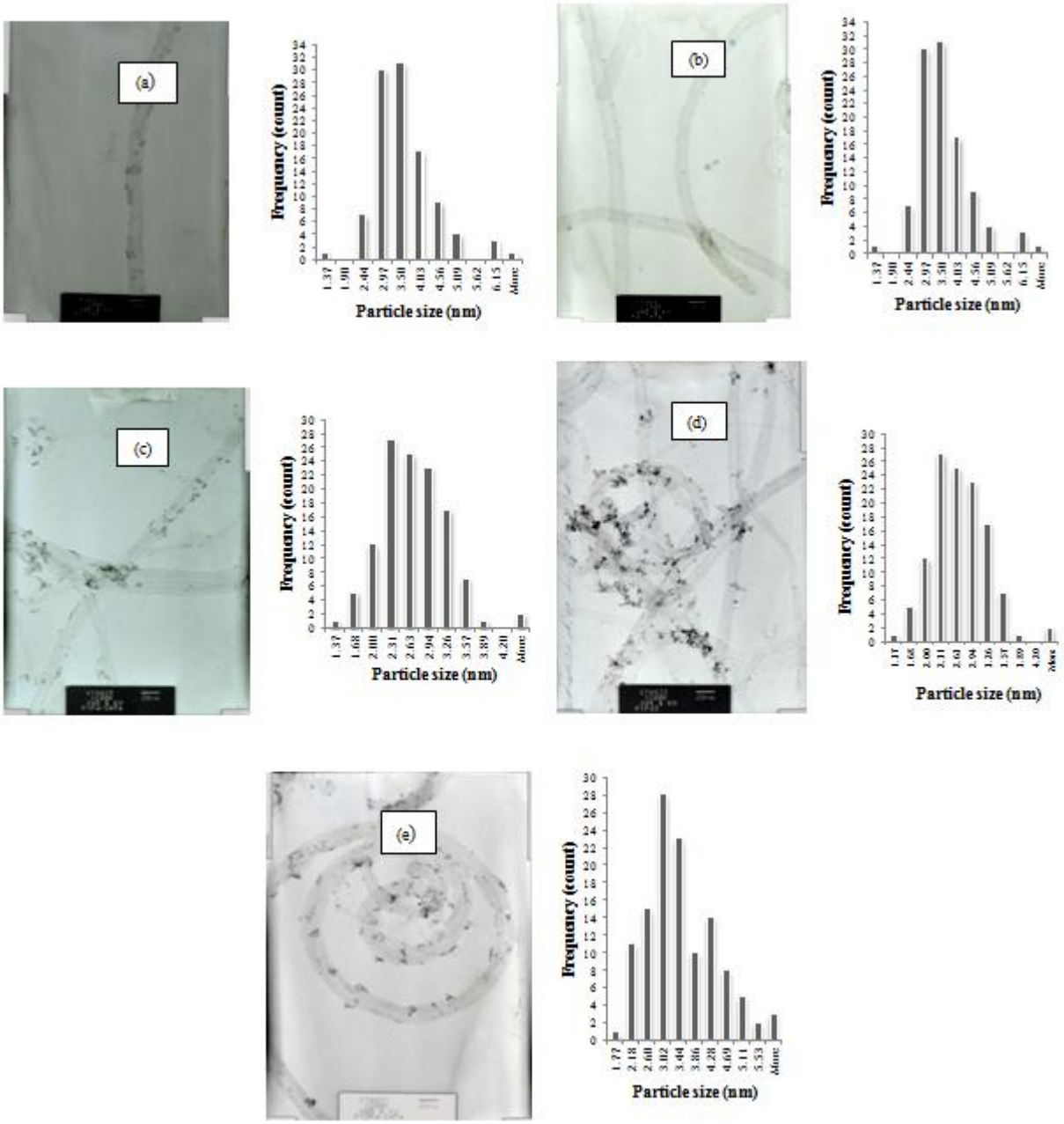


**Figure 2.** Representative TEM images and corresponding particle size histograms of a) Pt/CNTs, b) Pd/CNTs, c) PtPd/CNTs, d) $PtPd_3$/CNTs and e) $Pt_3Pd$/CNTs catalysts.

In Figure 2 shows the selected TEM micrographs of each catalysts and the histograms of the particle size distributions constructed by counting at least 100 particles on each catalyst with range of particle size 2 -4 nm. $Pt_xPd_y$ nanoparticles are well dispersed on functionalized CNT supports and aggregations were found in some area. TEM results of all nanoparticles are shown in Table 1.

**Table 1.** Characteristics and activity for formic acid oxidation on various catalysts.

| Electrocatalysts | Particle size (from TEM) | Onset Potential | Current density $i_{max}$(from CV) | Current density at 3600 $s^{-1}$(from CA) |
|---|---|---|---|---|
| | (nm) | (V) | ($mA/mg_{catalysts}$) | ($mA/mg_{catalysts}$) |
| Pt/CNTs | 1.67 ± 0.49 | 0.05 | 2500 | 10.80 |
| Pd/CNTs | 3.35 ± 0.86 | -0.15 | 430 | -0.63 |
| $PtPd_3$/CNTs | 2.56 ± 0.55 | -0.10 | 2400 | 8.41 |
| PtPd/CNTs | 2.75 ± 0.71 | -0.10 | 8000 | 29.09 |
| $Pt_3Pd$/CNTs | 3.27 ± 0.93 | -0.10 | 4500 | 23.53 |
| PtRu/C | - | 0.20 | 3.5 | 0.05 |

*3.2. Electrochemical characterization*

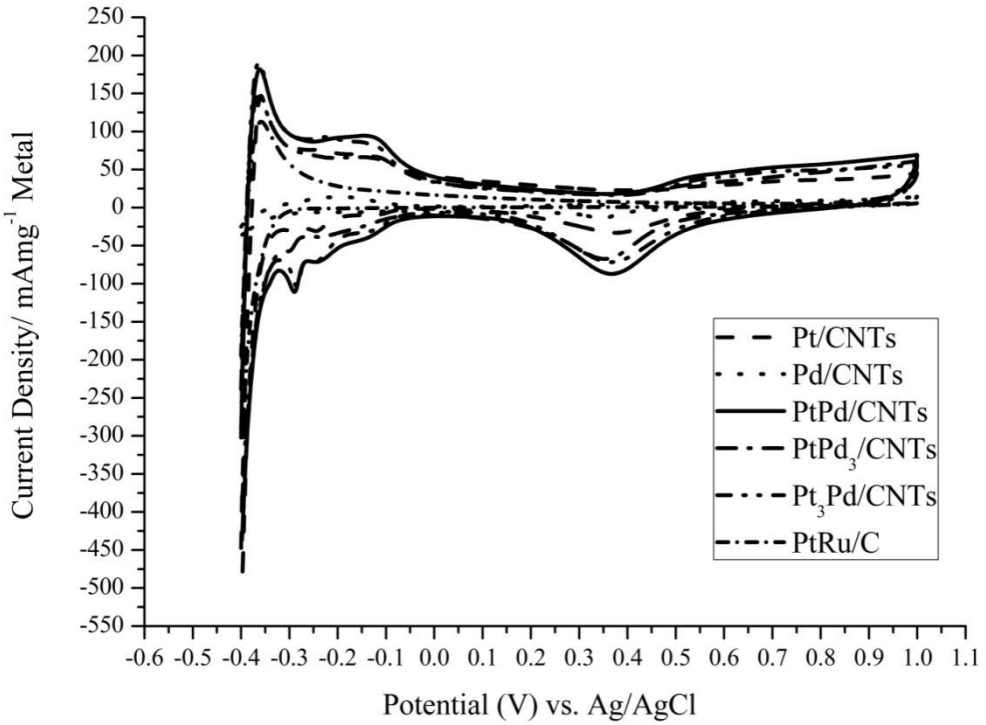


**Figure 3.** Cyclic voltammograms recorded in 0.5 M $H_2SO_4$ solution at Pt/CNTs, Pd/CNTs, PtPd/CNTs, $PtPd_3$/CNTs and $Pt_3Pd$/CNTs catalysts in the potential range -0.40 to 1.00 V at a scan rate 50 $mV.s^{-1}$.

Cyclic voltammograms of the $Pt_xPd_y$ /CNT catalysts in 0.5 M $H_2SO_4$ solution carried on in the range of -0.2 to 1.00 V (vs. Ag/AgCl) at a scan rate 50 $mV.s^{-1}$ are shown in Figure 3. The catalysts show the characteristic features of Pt and Pd in acid solution. The peaks appearing between -0.4 to -0.2 V are corresponding to atomic hydrogen adsorption/desorption at the surface of the catalyst in acid

media. All features are representative for catalysts in $H_2SO_4$ solution and in concurrence fit with previous report [6, 14, 18-20].

It is shown that PtPd/CNTs demonstrates excellent electrocatalytic activity mainly owing to the uniform distribution of the properly composition of the active catalyst nanoparticle with a narrow size distribution on the outer surface of the functionalized CNTs supporting materials. The high electrochemically active surface area of the PtPd/CNTs indicates that it could be an effective electrocatalysts for the formic acid oxidation.

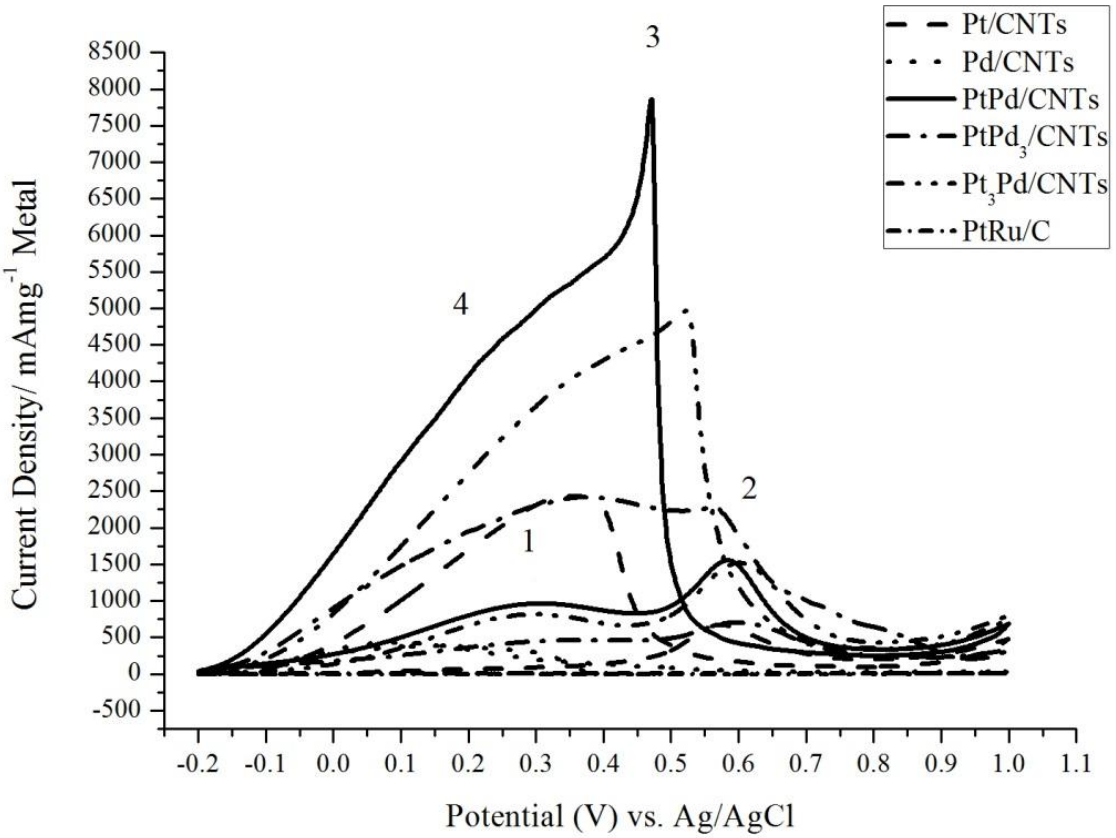


**Figure 4.** Cyclic voltammograms of Pt/CNTs, Pd/CNTs, PtPd/CNTs, $PtPd_3$/CNTs and $Pt_3Pd$/CNTs catalysts in the potential range -0.20 to 1.00 V with scan rate at 50 $mV.s^{-1}$ in 0.5 M $H_2SO_4$ in 0.5 M HCOOH solution.

To investigate the potential performance of catalysts whether or not they could be effective electrocatalysts for formic acid oxidation, the cyclic voltammograms were conducted in electrolyte of 0.5 M HCOOH in 0.5 M $H_2SO_4$ at the potential range -0.20 to 1.00 V vs. Ag/AgCl with a scan rate of 50 $mV.s^{-1}$. Figure 4 shows the cyclic voltammograms for of Pt/CNTs, Pd/CNTs, PtPd/CNTs, $PtPd_3$/CNTs and $Pt_3Pd$/CNTs catalysts in 0.5 M HCOOH in 0.5 M $H_2SO_4$ solution at the potential range -0.20 to 1.00 V vs. Ag/AgCl with a scan rate of 50 $mV.s^{-1}$. In the foreword scan, two peaks labeled as 1 and 2 are observed at ca. 0.30 and 0.60 V, respectively. In backward scan, two peaks labeled as 3 and 4 are obtained ca. 0.45 and 0.25 V, respectively. It was stated that formic acid oxidation on catalyst electrodes has $CO_2$ as main product in equation (1) and $CO_{ads}$ in equation (2) as

principal by-product. The anodic peak 1 can be attributed to HCOOH oxidation on the surface sites that stayed unblocked after $CO_{ads}$ adsorption. The anodic peak 2 $CO_{ads}$ oxidation was involved during the backward potential sweep; the surface remains inactive until the partial reduction of the oxide species formed. The oxidation peak 3 shows the real electrocatalytic activity of the catalyst surface, as no CO and oxide present in the surface. The shoulder peak 4 are attributed to oxide species is oxidized.

Two peaks are observed in the positive scan at anodic peak and the negative scan at cathodic peak, indicating that the oxidation of formic acid to carbon dioxide ($CO_2$) follows either direct path or dehydrogenation path [6,8].

Dehydrogenation $HCOOH \rightarrow CO_2 + 2H^+ + 2e^-$ (1)

Dehydration $HCOOH \rightarrow CO_{ads} + H_2O \rightarrow CO_2 + 2H^+ + 2e^-$ (2)

From onset potential and current intensity in Table 1, compared with commercial PtRu/C, PtPd/CNTs catalyst shows the lowest onset potential and highest current intensity which indicates an excellent electrocatalytic activity for formic acid oxidation.

*3.3. Electrocatalyst stability*

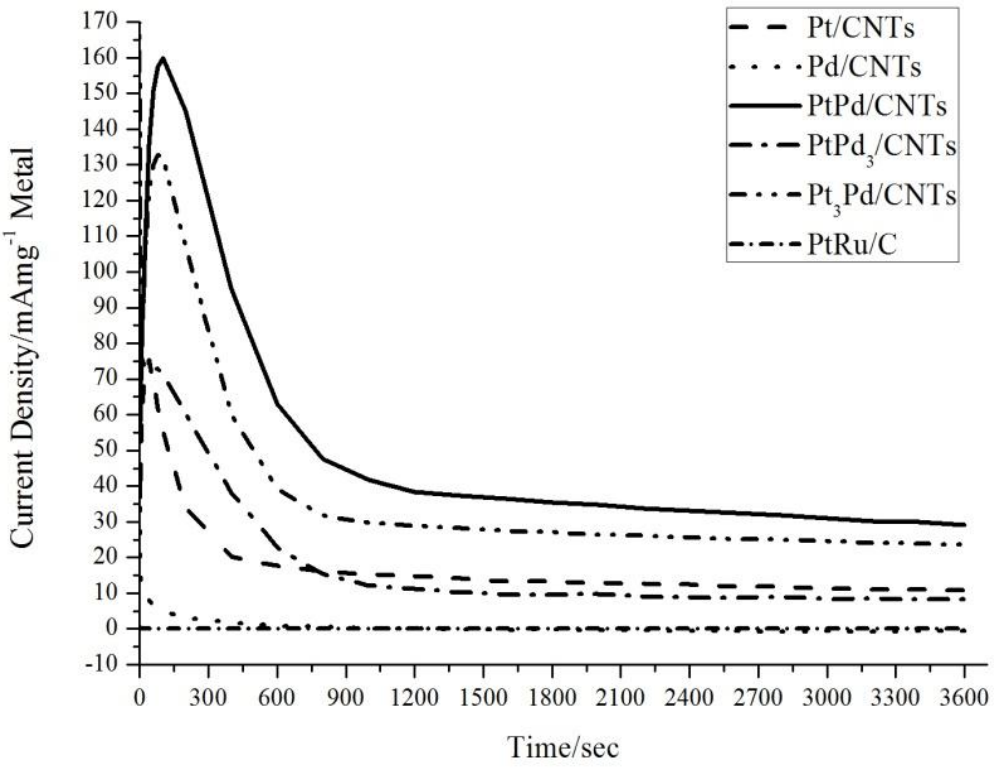


**Figure 5.** Chronoamperometric curves of Pt/CNTs, Pd/CNTs, PtPd/CNTs, $PtPd_3$/CNTs and $Pt_3Pd$/CNTs catalysts in 0.5 M HCOOH in 0.5 M $H_2SO_4$ solution at 0.30 V vs. Ag/AgCl for 3,600 second reaction time.

Electrocatalytic durability of the catalysts in 0.5 M HCOOH in 0.5 M $H_2SO_4$ solution by chronoamperometric (CA) curves recorded at 0.3 V for 3600 seconds are shown in Figure 5. The measurements are used to test the initial stability of the prepared catalysts. It can be seen that the formic acid oxidation current decreases continuously for all the catalysts, apparently due to catalysts poisoned by chemisorbed carbonaceous species formed during oxidation but the decay in the oxidation current with times is different[9,15]. The initial rapid decay in current density can most likely be ascribed to surface poisoning stimulated by intermediate species formed on the catalyst surface. This significant electrocatalytic activity and stability is anticipated from higher surface area of the functionalized CNT support which maintains high dispersion and small nanoparticle size of the electrocatalyst. The $Pt_xPd_y$/CNTs catalyst was found to have the most excellent electrocatalytic performance and improved durability. The CA curves of the PtPd/CNTs (Figure 5) remains higher than the other catalysts which indicates that the PtPd/CNTs has better electrocatalytic activity and stability for formic acid oxidation during the experimental time period. Therefore, the catalysts prepared by our improved polyol method are more likely to be used as electrocatalyst in formic acid fuel cells.

## 4. CONCLUSIONS

Catalysts loaded functionalized CNTs surface were prepared by improved polyol methods and performed for the electrocatalytic study in formic acid oxidations. The prepared metal catalyst nanoparticle dispersed on the functionalized CNTs with mean particle sizes of ca. 2-4 nm were obtained. Pt and Pd in CNTs matrix can enhance the current intensities for formic acid oxidations. Cyclic voltammograms show that formic acid oxidation current density at PtPd/CNTs electrode is higher than that of the commercial PtRu/C catalyst and the other prepared catalysts. Moreover, the amperometric i – t results also show that PdPt/CNTs catalyst is more stable than others. These improvements in electrocatalytic activity and stability provide opportunity of the PtPd/CNTs for applications in direct formic acid fuel cell.

ACKNOWLEDGEMENTS
The authors would like to thank, the National Research University Project under Thailand's Office of the Higher Education Commission and Center of Excellence for Innovation in Analytical Science and Technology, Faculty of Science, Chiang Mai University for financial support.

## References

1. C. Rice, S. Ha, R. I. Masel , P. Waszczuk, A. Wieckowski and T. Barnard, *J. Power Sources*, 111 (2002) 83.
2. A. Capon and R. Parsons, *J. Electroanal. Chem. Interfacial Electrochem.*, 44 (1973) 239.
3. S. Uhm, H. J. Lee and J. Lee, *Phys. Chem. Chem. Phys.*, 11 (2009) 9326.
4. X. Yu and P. G. Pickup, *J. Power Sources*, 182 (2008) 124.
5. C. Rice, S. Ha, R. I. Masel and A. Wieckowski, *J. Power Sources*, 115 (2003) 229.

6. M. Arenz, V. Stamenkovic, T. J. Schmidt, K. Wandelt, P. N. Ross and N. M. Markovic, *Phys. Chem. Chem. Phys.*, 5 (2003) 4242.
7. O. A. Petrii, *J. Solid State Electrochem.*, 12 (2008) 609.
8. Z. Liu , L. Hong, M. P. Tham, T. H. Lim and H. Jiang, *J. Power Sources*, 161 (2006) 831.
9. E. Antolini, *Mater. Chem. and Phys.*, 78 (2003) 563.
10. A. O. Al-Youbi, J. L. Gómez de la Fuente, F. J. Pérez-Alonso, A. Y. Obaid, J. L. G. Fierro, M. A. Peña, M. Abdel Salam and S. Rojas, *Appl. Catal. B*, 150-151 (2014) 21.
11. P. Serp, M. Corrias and P. Kalck, *Appl. Catal. A*, 253 (2003) 337.
12. G. Wu and B. Q. Xu, *J. Power Sources*, 174 (2007) 148.
13. Z. He, J. Chen, D. Liu, H. Zhou and Y. Kuang, *Diamond Relat. Mater.*, 13 (2004) 1764.
14. W. Qian, R. Hao, J. Zhou, M. Eastman, B. A. Manhat, Q. Sun, A. M. Gofort and J. Jiao, *Carbon*, 52 (2013) 595.
15. O. Winjobi, Z. Zhang, C. Liang and W. Li, *Electrochim. Acta.*, 55 (2010) 4217.
16. Y. Liu, M. Chi, V. Mazumder, K. L. More, S. Soled, J. D. Henao and S. Sun, *Chem. Mater.*, 23 (2011) 4199.
17. A. B. A. A. Nassr, A. Quetschke, E. Koslowski and M.Bron, *Electrochim. Acta.*, 102 (2013) 202.
18. J. D. Lović, A. V. Tripković, S. L. Gojković, K. D. Popović, D. V. Tripković, P. Olszewski and A. Kowel, *J. Electroanal. Chem.*, 581 (2005) 294.
19. M. Rahsepar, M. Pakshir, Y. Piao and H. Kim, *Fuel Cells*, 12 (2012) 827.
20. N. V. Long, M. Ohtaki, T. D. Hien, J. Randy and M. Nogami, *Electrochim. Acta.*, 56 (2011) 9133.